Corresponding author:
Hayato Abe (Kyushu University): ORCID: 0000-0001-6092-0130. Twitter (X): HayatoABE3 (https://x.com/HayatoABE3)

Title

Sensitivities of soil respiration and heterotrophic respiration to temperature in a cool-temperate forest with sika deer-induced understory vegetation alteration

Authors and affiliations

Hayato Abe [(1)]*, Tomonori Kume [(2)], Ayumi Katayama [(3)]

(1) Graduate School of Bioresource and Bioenvironmental Sciences, Kyushu University, Fukuoka-city, Fukuoka 819-0395, Japan. E-mail: abe.hayato.360@s.kyushu-u.ac.jp

(2) Kasuya Research Forest, Kyushu University, Sasaguri-town, Fukuoka 811-2415, Japan. E-mail: kume.tomonori.329@m.kyushu-u.ac.jp

(3) Shiiba Research Forest, Kyushu University, Shiiba-village, Miyazaki 883-0402, Japan. E-mail: katayama.ayumi.462@m.kyushu-u.ac.jp

13 *Corresponding author: Hayato Abe, Tel. +81-92-948-3103, Fax. +81-92-948-3127,
14 Kasuya Research Forest, Kyushu University, Sasaguri-town, Fukuoka 811-2415,
15 Japan

16 **Keywords**

17 Overgrazing, Understory degradation, Forest type, Succession, Cervus nippon

18 **Running title**

19 Temperature sensitivity of soil respiration under different forest understories

Abstract

Overpopulated ungulates reduce the biomass of understory vegetation and promote the expansion of unpalatable plants in world forests. These understory degradations possibly influence sensitivities of soil respiration (R_s) and heterotrophic respiration (R_h) to temperature and moisture. Here, we examined this possibility in a cool-temperate forest in southern Kyushu, Japan. At the study site, the dominant understory vegetation, dwarf bamboo (Sasa; *Sasamorpha borealis*), has been lost and replaced by an unpalatable shrub, Asebi (*Pieris japonica*), owing to sika deer feeding. We targeted three understory vegetation types, namely, Sasa understory (SU), no understory (NU), and Asebi understory (AU). The R_s, R_h, soil temperature, and soil volumetric water content (SVWC) were measured at three points in each understory type using an automatic opening/closing chamber system from August 2022 to November 2023. We also evaluated understory conditions such as surface litter amount, fine root biomass, and soil physio-chemical properties to explore factors influencing the temperature sensitivity proxy (Q_{10}) of R_s and R_h. The temporal variation of R_s and R_h was affected strongly by soil temperature and weakly by SVWC for all understory types. Differences in Q_{10} among SU, NU, and AU were comparable to the differences in Q_{10} among measurement points within the same understory type. Spatial variation in Q_{10} of R_s and R_h was explained by fine root biomass and surface litter amount, respectively. There were no differences in fine root biomass and surface litter amount among understory types. The lack of difference in surface litter amount can be explained by the minimal litter runoff associated with the alteration from SU to NU and AU due to the flat topography. Our findings indicate that understory loss and species replacement caused

by deer do not affect the sensitivity of R_s or R_h at our site, which is characterized by flat topography.

1. **Introduction**

Sequestration of carbon dioxide (CO_2) is a crucial function of forest ecosystems under global warming. Recently, ungulate populations have increased in forests worldwide (Wilson and MacLeod, 1991; Coomes *et al.*, 2003; Takatsuki, 2009; Tape *et al.*, 2016; Guerisoli and Pereira, 2020). Non-uniform, excessive, and prolonged understory vegetation feeding by overpopulated ungulates (hereafter referred to as overbrowsing) has reduces the biomass and species diversity of understory vegetation (Hernández and Silva-Pando, 1996; Horsley *et al.*, 2003; Kato and Okuyama, 2004; Tremblay *et al.*, 2006; Suzuki *et al.*, 2008; Harada *et al.*, 2020). In addition, overbrowsing increases the abundance of plant species unpalatable for an ungulate diet (Enoki *et al.*, 2017; Abe *et al.*, 2024b; Tokumoto and Katayama, 2024). Such understory degradation potentially degrades forest carbon sequestration, for example, through an increase in carbon emissions from the forest (Ramirez *et al.*, 2018; Schmitz *et al.*, 2018; Forbes *et al.*, 2019; Leroux *et al.*, 2020). Further research examining this possibility is necessary to implement forest management practices that reduce carbon emissions under global warming and overbrowsing.

Soil respiration (R_s) is an important CO_2 efflux pathway in forest ecosystems. R_s comprises respiration by living roots and the associated rhizosphere (autotrophic respiration; R_a) as well as respiration by microbes through the decomposition of surface litter and soil organic matter (SOM) (heterotrophic respiration; R_h) (Bond-Lamberty and Thomson, 2010). Both R_s and R_h respond to temperature and moisture (Webster *et al.*, 2009). Thus, evaluation of the sensitivities of R_s and R_h to temperature and moisture, together with factors responsible for their variation, is important to clarify whether

68 overbrowsing-induced understory degradation impacts carbon-release processes in
69 forest ecosystems. However, current knowledge of the effect of understory vegetation
70 on the sensitivity of R_s and R_h to temperature and moisture is limited. Previous studies
71 have mainly conducted understory removal experiments (Yashiro *et al.*, 2012; Li *et al.*,
72 2019; Jing *et al.*, 2021; Zhao *et al.*, 2022) and detected no difference in the temperature
73 sensitivity of R_s and R_h between stands with and without understory vegetation.
74 Nevertheless, the underlying factors contributing to these results remain poorly
75 understood.

76 Temperature and moisture sensitivities of R_s and R_h vary with soil properties, such as
77 root production, soil bulk density (BD), and soil carbon concentration (SC) (Bond-
78 Lamberty and Thomson, 2010; Hursh *et al.*, 2017; Tang *et al.*, 2020; Jian *et al.*, 2022).
79 Loss of understory vegetation by overbrowsing impacts soil properties, including fine
80 root production (Ruess *et al.*, 1998), soil microorganism activities (Niwa *et al.*, 2011;
81 Chen *et al.*, 2023; Kadowaki *et al.*, 2023; Tokumoto *et al.*, 2024), and the amounts and
82 decomposability of surface litter and SOM (Kooijman and Smit, 2001; Binkley *et al.*,
83 2003; Kawakami *et al.*, 2020a, 2020b; Katayama *et al.*, 2023). In addition, the
84 replacement of understory vegetation by unpalatable plant species through
85 overbrowsing affects these soil properties (Harada *et al.*, 2020; Ohira *et al.*, 2022; Abe
86 *et al*., 2024b). Thus, loss and species replacement of understory vegetation by
87 overbrowsing may alter the temperature and moisture sensitivities of R_s and R_h through
88 the changes in soil properties.

89 Currently, the population size of sika deer (*Cervus nippon*) has reached its
90 historically highest level in the Japanese archipelago (Iijima *et al.*, 2023). In southern

Kyushu Island, the dominant understory vegetation, dwarf bamboo (Sasa; *Sasamorpha borealis*) (Fig. 1a), has been decreasing and disappearing as a result of the overbrowsing since the 1980s (Fig. 1b) (Saruki *et al.*, 2004). In addition, overbrowsing has led to the replacement of Sasa by the unpalatable shrub, Asebi (*Pieris japonica*) (Fig. 1c) (Enoki *et al.*, 2017; Tokumoto and Katayama, 2024). In this study, we aimed to examine whether the understory loss and species replacement caused by deer affect the sensitivity of R_s or R_h. For this aim, we conducted field measurements of R_s and R_h in a cool-temperate forest with three types of understory vegetation (i.e., Sasa understory, no understory, and Asebi understory).

2. Material and methods

2. 1 Study site and experimental design

This study was conducted in Kyushu University Shiiba Research Forest (SRF), located in southern Kyushu Island (32°20′53″N, 131°5′32″E, 880 m above sea level). The mean annual temperate (MAT) and precipitation (MAP) in the study area were 10.8 ℃ and 3207.9 mm, respectively (DEIMS-SDR, 2021). The study site was on flat terrain with a slope of <5 degrees. We established a study plot with an area of 600 m^2 on March 2, 2024. In the study plot, species name and diameter at breast height (DBH) were recorded for overstory trees with DBH >3 cm. The mean and standard deviation (SD) of DBH were 18.4 ± 9.7 cm. The stem density was 683.6 stems $ha^{-1,}$ and the basal area was 23.0 m^2 ha^{-1}. The dominant species were *Quercus variabilis*, *Q. crispula*, and *Q. serrata*. These three species comprised 85.4% of the stem density and 83.6% of the basal area.

Before overbrowsing, the understory vegetation in SRF was entirely covered by Sasa (i.e., *S. borealis*). Due to the overbrowsing since the 1980s, Sasa has decreased (Saruki *et al.*, 2004), and the population of Asebi has increased (Enoki *et al.*, 2017; Ichihashi and Katayama, 2024; Tokumoto and Katayama, 2024). We targeted three understory types within the study plot: Sasa understory (SU, Fig. 1a), no understory (NU, Fig. 1b), and Asebi understory (AU, Fig. 1c). SU was located within areas enclosed by deer exclusion fences, and was considered to be the baseline understory type (Abe et al., 2024b; Tokumoto *et al.*, 2024). NU and AU were located outside the fenced areas and were considered to be overbrowsing-induced understory types (Abe *et*

122 *al.*, 2024b). AU developed from NU at the site with high light availability due to the
123 expansion of Asebi (Tokumoto and Katayama, 2024).

124 We established three CO_2 efflux measurement points of R_s and R_h in each
125 understory type (i.e., two-soil respiration components × three-understory types × three-
126 point replications = 18 points) on March 16, 2022. We installed short polyvinyl chloride
127 (PVC) collars at each point to measure R_s. We employed a micro-trenching method to
128 measure R_h (Riutta *et al.*, 2021); for this method, tall PVC collars were installed at each
129 measurement point. The diameter of the PVC collars was 11 cm, with a height of 10 cm
130 for the short collars and 45 cm for the tall collars. Installed PVC collars were exposed 5
131 cm above the ground surface. The roots inside the tall PVC collars were cut to install
132 the tall PVC collars. Hence, R_h in this study excludes CO_2 efflux from living roots and
133 the associated rhizosphere at 0–40 cm depth (Riutta *et al.*, 2021). The collars were
134 allowed to stabilize for 18 weeks before the data collection started. Previous studies that
135 used the micro-trenching method have shown that CO_2 efflux in tall PVC collars
136 stabilized within 1 week (Sapronov and Kuzyakov, 2007; Thurgood *et al.*, 2014; Riutta
137 *et al.*, 2021).

138 **2.2 Vegetation and soil property census**

139 To estimate understory vegetation biomass, we installed a 0.5 m × 0.5 m frame
140 surrounding each CO_2 efflux measurement point. On March 2, 2024, we measured the
141 number of culms of Sasa, the culm height of Sasa, and the diameter at 5 cm height (D_5,
142 cm) of Asebi inside the frame. The biomass of Sasa was estimated using the following
143 equation:

$$B = 15.928NH + 335.000 \quad (1)$$

where B is the biomass of Sasa (g m^{-2}), N is the number of culms of Sasa (m^{-2}), and H is the culm height of Sasa (m). This equation was created from the results of understory harvesting survey in SRF (Abe *et al.*, 2024b) (Fig. S1). The biomass of Asebi was estimated using an allometric equation established in SRF (Ichihashi and Katayama, 2024):

$$\log_{10}(W) = 2.255 \log_{10}(D_5) + 1.533 \quad (2)$$

where W is the individual biomass of Asebi (g). The total value of W in each frame was divided by the frame size (0.025 m^2) to obtain area-based biomass (g m^{-2}).

To investigate the soil properties, we measured surface litter amount (g m^{-2}), fine root biomass (g m^{-2}), SOM amount (g C m^{-2}), BD (g m^{-3}), and SC (g C g^{-1}) on March 2, 2024. The surface litter included leaf litter and fine woody debris with a diameter of approximately <3 cm (Abe *et al.*, 2022b). Fine roots included all living plant roots with a diameter of <2 mm. We sampled surface litter inside 0.3 m × 0.3 m frames placed near the measurement points. Surface litter was separated into Sasa, Asebi, and other tree species. Surface litter that had decomposed to inseparability was classified as inseparable. Surface litter was oven-dried at 70 °C for 48 h and weighed. We sampled soil cores to determine fine root biomass, BD, and SC. This was performed around all measurement points at 0–5 cm and 5–10 cm depths. After the removal of surface litter, we used a 100 ml syringe to collect soil cores in three positions at each measurement point. The soil core samples were pooled for each measurement point and sieved through a 2 mm mesh, and then mineral soil and fine roots were separated. The fine roots were further separated into

166 Sasa, Asebi, and other tree species. No inseparable roots were present. Mineral soil and
167 fine roots were oven-dried at 70 °C for 48 h and weighed. BD was determined by dividing
168 the mass of mineral soil (g) by the sample volume (0.0003 m^{-3}). SC was measured using
169 a C/N corder (Macro Corder JM1000CN, J-Science Lab Co., Kyoto, Japan). SOM amount
170 was calculated by multiplying BD, SC, and the sampling depth of each soil layer (0.05
171 m).

172 **2.3 Soil respiration measurement**

173 We measured R_s and R_h at each measurement point using a closed static chamber
174 (HL-1019A, Fuxin Gongda Hualian Technology Co., Ltd., Liaoning, China) (Kuriyama
175 *et al.*, 2021; Wang *et al.*, 2022). The chamber system consisted of a cylindrical chamber
176 (soil exposure area: 165 cm^2, chamber volume: 3300 cm^3), an infrared gas analyzer, and
177 a fan that circulates the air in the chamber in one unit. A thermometer measured the gas
178 temperature in the chamber. Measurements of CO_2 concentration and gas temperature
179 were recorded at 3-second intervals over 7.5 min. The CO_2 efflux (F, μmol m^{-2} s^{-1}) was
180 calculated as follows:

181 $$\boldsymbol{F} = \frac{dc}{dt} \times \frac{V_s}{V_a} \times \frac{273.15}{(273.15+ T_a)} \times \frac{1}{A} \quad (3)$$

182 where dc/dt is the CO_2 concentration increment per second (μmol mol^{-1} s^{-1}), V_s is the
183 volume of the chamber (3.3 L), V_a is the standard molar volume of the atmosphere (22.4
184 L mol^{-1}), T_a is the gas temperature (°C), and A is the soil exposure area (0.0165 m^2).
185 After the measurement period, the movable partition opened and automatically
186 exhausted the air from the chamber. The system automatically recorded CO_2 efflux at
187 20-minute intervals, including the exhaust period. In each recording period, soil

temperature (°C) and soil volumetric water content (SVWC, %) at 5 cm depth near the chamber were automatically measured from a thermometer and a time domain reflectometer sensor. Measurements were conducted during six campaigns from 2022 to 2023 (August 5 to October 6, 2022; November 14 to December 4, 2022; February 14 to February 28, 2023; March 14 to April 10, 2023; July 10 to August 31, 2023; and October 30 to November 8, 2023). In each campaign, two chambers were used to measure CO_2 efflux at one short PVC collar and one tall PVC collar per day.

2.4 Soil respiration modeling

We examined the relationships of R_s and R_h with soil temperature and SVWC for each understory type. This was done using three empirical equations. The first equation expresses the exponential relationship using soil temperature (Lloyd and Taylor, 1994):

$$F = \mathrm{a}\exp(\mathrm{b}T) \quad (4)$$

where T is soil temperature (°C) at 5 cm depth, and a and b are constants. The second equation expresses quadric relationships using SVWC (Saiz *et al.*, 2006):

$$F = \mathrm{c}+\mathrm{d}\theta + \mathrm{f}\theta^2 \quad (5)$$

where θ is SVWC (%) at 5 cm depth, and c, d, and f are constants. The third equation expresses the exponential-power relationships using T and θ (Saiz *et al.*, 2006):

$$F = \mathrm{g}\exp(\mathrm{h}T)\,\theta^{\mathrm{i}} \quad (6)$$

where g, h, and i are constants. To estimate the constants in Eqs. 4–6, non-linear mixed-effect models (Lindstrom and Bates, 1990) were applied to pooled data from the three

measurement points for each understory type. Thus, all constants in Eqs. 4–6 consisted of fixed and random effects. Fixed effects were expressed as representative constants in each understory type. Random effects were assigned to differences of measurement points in each understory type. Constants were fitted using a maximum likelihood procedure. The goodness of fit was evaluated with the Akaike information criterion (AIC), and the coefficient of determination was explained by fixed effects (Marginal R^2) (Spiess and Neumeyer, 2010). The analyses were conducted using R software version 4.2.2 for Windows 10 x64 (R Core Team, 2024) with the packages "nlme" (Pinheiro *et al.*, 2017) and "nlraa" (Miguez, 2021).

We calculated Q_{10} to determine the temperature sensitivity of R_s and R_h as follows (Lloyd and Taylor, 1994):

$$Q_{10} = \exp(10b) \quad (7)$$

where b is the constant in Eq. 4. Representative Q_{10} in each understory type was calculated based solely from the fixed effects of constant b. In addition, the spatial variation of Q_{10} was evaluated as the SD of Q_{10} between measurement points in each understory type. Q_{10} in each measurement point was calculated from constant b at each measurement point, which is the sum of fixed effects and point-specific random effects.

2.5 Statistical tests

We used the Tukey honest significant differences test to assess whether understory vegetation biomass, surface litter amount, fine root biomass, SOM amount, BD, and SC varied among different understory types. In addition, the effects of these variables on the Q_{10} of R_s and R_h were evaluated by linear regression analysis. This regression

analysis targeted Q_{10} values for each measurement point. The significance threshold for statistical tests was set at $p < 0.05$. These analyses were conducted in R software with packages “stats” (R Core Team, 2024) and "multicomp" (Bretz *et al.*, 2010).

3. Results

3.1 Soil characteristics

The understory vegetation biomass in SU was 26-fold higher than that in NU and 5-fold higher than that in AU (Table 1, Table S1). No differences in surface litter amount were detected among SU, NU, and AU. At each measurement point, overstory trees contributed 92%–98%, 100%, and 51%–84% of the total surface litter in SU, NU, and AU, respectively (Fig. S2). No differences in fine root biomass were observed at any depth among SU, NU, and AU. Nevertheless, Sasa and Aesbi contributed 23%–35% and 42%–63% of fine root biomass at 0–10 cm depth in SU and AU, respectively (Fig. S3). The SOM at 0–5 cm and 0–10 cm depth in NU were 1.51- and 1.15-fold higher than in SU and AU, respectively. Although this was due to the relatively higher BD in NU than in SU and AU, differences in BD were not significant at any depth. In addition, no differences in SC were detected at any depth among SU, NU, and AU.

3.2 Estimated soil temperature and moisture models for soil respiration

A consistent positive exponential response of R_s and R_h to soil temperature was observed for all understory types (Fig. 2). The R^2 values for the temperature model (i.e., Eq. 4) ranged from 0.84 to 0.92, suggesting that most of the variation in R_s and R_h was explained by soil temperature (Table 2). Unimodal responses of R_s and R_h to SVWC was detected, except for R_h in SU and R_s in AU (Fig. S4). Despite of this, the R^2 values for the SVWC model (i.e., Eq. 5) were less than 0.5 (0.015 to 0.48; Table 2). Furthermore, the AIC and R^2 values for the hybrid model of temperature and SVWC (i.e., Eq. 6) did not differ from those of the temperature model (e.g., the results in SU

had AIC = −5439.92 and R^2 = 0.84 for the temperature model, and AIC = −5611.54 and R^2 = 0.88 for the hybrid model; Table 2).

The Q_{10} calculated solely from the fixed effects, as well as the SD of Q_{10} in each measurement point, were as follows. Q_{10} of R_s was 2.42 ± 0.31 for SU, 2.50 ± 0.19 for NU, and 2.60 ± 0.34 for AU. The Q_{10} of R_h was 2.73 ± 0.07 for SU, 3.00 ± 0.52 for NU, and 3.17 ± 0.33 for AU. For R_s and R_h, differences in Q_{10} among understory types were only as large as the SD of each measurement point.

Surface litter amount was positively related to the Q_{10} of R_h (Table 3, Fig. 3). Fine root biomass at 0–10 cm and 0–5 cm depth was positively related to the Q_{10} of R_s (Fig. 4). The SOM amount, BD, or SC were not related to Q_{10} of R_s and R_h.

4. Discussion

The temporal variations of R_s and R_h were affected strongly by soil temperature and weakly by SCWC (Table 2). This result was in line with most previous studies that indicated the temporal variation of R_s and R_h is controlled primarily by soil temperature (e.g., Chen *et al.*, 2020). The possible reason for the lower sensitivity of SVWC is the climatic conditions at the present study site. The sensitivities of R_s and R_h to SVWC are higher in dry areas than in wet areas (Manzoni *et al.*, 2012; Liu *et al.*, 2016; Morris *et al.*, 2022). For instance, in arid grasslands, R_s is more sensitive to SVWC than to soil temperature; therefore, ungulate browsing significantly alters R_s sensitivity to SVWC (Jia *et al.*, 2006). The MAP in the present study area was 3207.9 mm, indicating that the soil is always well-moistened. Therefore, the present study area showed lower sensitivities of R_s and R_h to SVWC despite the different understory types.

The Q_{10} of R_s and R_h differed slightly among SU, NU, and AU. The similarity in Q_{10} of R_s and R_h between SU and NU aligns with previous findings that understory vegetation removal does not change Q_{10} in other temperate forests (Yashiro *et al.*, 2012; Li *et al.*, 2019). Furthermore, Q_{10} values in three present understory types were within the range of Q_{10} values in the global forest ecosystem dataset (Chen *et al.*, 2020) (Fig. S5). Except for three outliers (12.18 and 13.46 for Q_{10} of R_s and 20.45 for Q_{10} of R_h), this dataset showed that the Q_{10} of R_s and R_h ranged from 0.98 to 7.39 and 1.15 to 6.24, respectively. In addition, Q_{10} of R_s decreased consistent with MAT ($Q_{10} = 3.70 - 0.0848 \times$ MAT, adjusted $R^2 = 0.23$, $p < 0.001$), and Q_{10} of R_h was not related to MAT ($p = 0.614$). The Q_{10} of R_s in the present study (2.42–2.60) was comparable to the same MAT range ($Q_{10} = 2.78$ at 10.8 °C) for all understory vegetation types (Fig. S5a). The

288 Q_{10} of R_h (2.73–3.17) was also similar to the overall average of the dataset (2.68, Fig.
289 S5b).

290 Surface litter amount positively affected spatial variation in Q_{10} of R_h (Fig. 3). This
291 result aligns with previous reports that litter addition increases, and litter removal
292 decreases, the Q_{10} of R_h (Liu *et al.*, 2022; Zhuang *et al.*, 2023). Surface litter provides
293 additional substrate and increases microbial biomass, which in turn enhances the Q_{10} of
294 R_h (Zhuang *et al.*, 2023). The priming effect, whereby the addition of fresh organic
295 matter stimulates the decomposition of older organic matter, can also increase the Q_{10} of
296 R_h (Liu *et al.*, 2020). Although the surface litter of Sasa and Asebi were expected to
297 differ in degradability from the litter of tree species (Watanabe *et al.*, 2013; Tokumoto
298 and Katayama, 2024), the effect might be minimal because Sasa and Asebi accounted
299 for a small percentage of the surface litter in SU and AU (Fig. S2).

300 Fine root biomass positively affected spatial variation in Q_{10} of R_s (Fig. 4). This result
301 is consistent with previous findings that fine root biomass explains the spatial variability
302 of Q_{10} in R_s (Franck *et al.*, 2011; Luan *et al.*, 2013; Han and Jin, 2018). Root biomass
303 explains the spatial variation in R_s (Behera *et al.*, 1990; Rodeghiero and Cescatti, 2006;
304 Ceccon *et al.*, 2011; Comeau *et al.*, 2018; Abe *et al.*, 2022c). R_a is more temperature-
305 sensitive than that from bulk soil (Boone *et al.*, 1998; Epron *et al.*, 2001; Saiz *et al.*,
306 2006; Ruehr and Buchmann, 2009; Tomotsune *et al.*, 2013). The combination of root
307 biomass and higher Q_{10} of R_a can increase the Q_{10} of R_s. Furthermore, higher root
308 biomass can indirectly contribute to R_s through the decomposition of dead roots (Saha *et*
309 *al.*, 2023) and stimulation of SOM decomposition (Adamczyk *et al.*, 2019). Although
310 root species composition differed with understory type in the present study (Fig. S3),

311 total fine root biomass did not change (Table 1). Thus, the present results suggested that
312 the variability of R_s of Q_{10} at the study site was mainly regulated by fine root biomass
313 and was not affected by root species composition.

314 The similarity in Q_{10} of R_s and R_h among understory types was caused by the lack
315 of differences in surface litter amount and fine root biomass, respectively (Table 1). Abe
316 *et al.* (2024b) conducted a vegetation and soil properties census for SU, NU, and AU in
317 forests 3–10 km distant from the present study site. This previous study reported no
318 change in understory vegetation biomass and fine root biomass, supporting the present
319 results and inferences. However, the surface litter amount was reduced because of
320 overbrowsing in the previous study site. This finding was inconsistent with the present
321 results. The previous study site was located on a steep slope of 7.9–37.3°, on which
322 severe soil erosion had occurred (Abe *et al.*, 2022a, 2024a). In contrast, the present
323 study site was located on a flat terrain with a slope of less than 5°, where reduction in
324 surface litter associated with soil erosion was unlikely. This suggests that the impact of
325 alteration in understory vegetation by overbrowsing on the Q_{10} of R_h may be mediated
326 by site erodibility. In particular, the Q_{10} of R_h on steep slope terrain may decrease
327 because of the loss of surface litter by soil erosion.

5. Conclusions

This study examined the influence of alteration in understory type by overbrowsing on the temperature and moisture sensitivities of R_s and R_h. Despite the loss and species replacement of understory vegetation caused by overbrowsing, this only slightly impacted the Q_{10} of both R_s and R_h. This is because the surface litter amount and fine root biomass, which determine the spatial variability of Q_{10}, remained unchanged among different understory types. The relationship of surface litter and fine roots with Q_{10} of R_s and R_h has been relatively underexplored compared with other soil properties, such as SOM amount and SC (Bond-Lamberty and Thomson, 2010; Hursh *et al.*, 2017; Chen *et al.*, 2020; Tang *et al.*, 2020; Jian *et al.*, 2022). Given that surface litter and fine roots could serve as proxies for understory types (Zhang *et al.*, 2022; Deng *et al.*, 2023), future research should focus on the relationship between these factors and soil respiration.

It should be noted that the conclusions of the present study are based on findings in forests on flat terrain and moist soils. Climatic and topographical factors may influence the impact of understory types on soil respiration (Ohashi *et al.*, 2008). Accumulation of site-based knowledge is essential to generalize the results of the present study. This research will contribute to the formulation of forest management practices that reduce local carbon emissions under global warming and overbrowsing.

Acknowledgments

This work was supported by the JSPS KAKENHI (grant numbers 22KJ2456, 21H05316, 20H02684). We acknowledge the staff of the SRF for permitting us to conduct the research, and managing the study site. We thank Robert McKenzie, PhD, from Edanz (https://jp.edanz.com/ac) for editing a draft of this manuscript.

Conflict of interest

We declare that the research was conducted in the absence of any commercial or financial relationships that could be construed as a potential conflict of interest.

Authors contributions

AH contributed to conceptualization, funding acquisition, investigation, data analysis, and drafted the original manuscript. KT contributed to funding acquisition, investigation, and revision/editing of the manuscript. KA contributed to the supervision, conceptualization, funding acquisition, investigation, and revision/editing of the manuscript.

Data availability

The point-level data, including Q_{10} of R_a and R_h, as well as understory conditions, is available in Table S1 in supplementally materials. More detailed data will be made available upon request.

365 **References**

366 Abe H, Fu D, Kume, T *et al.*, 2022a: Exposure of tree roots and its control factors in a
367 mixed temperate forest with no understory vegetation. *Bulletin of the Kyushu University*
368 *Forest* **103**, 13–20. doi:10.15017/4776829 (Japanese with English summary).

369 Abe H, Katayama A, Taniguchi S *et al.*, 2022b: Effects of differences in aboveground
370 dead organic matter types on the stand-scale necromass and CO_2 efflux estimates in a
371 subtropical forest in Okinawa Island, Japan. *Ecological research* **37**, 609–622.
372 doi:10.1111/1440-1703.12317.

373 Abe H, Kume T, Hyodo F *et al.*, 2024a: Soil erosion under forest hampers beech
374 growth: Impacts of understory vegetation degradation by sika deer. *Catena* **234**,
375 107559. doi:10.1016/j.catena.2023.107559.

376 Abe H, Kume T, Katayama A, 2024b: Reduction in forest carbon stocks by sika deer-
377 induced stand structural alterations. *Forest ecology and management* **562**: 121938.
378 doi:10.1016/j.foreco.2024.121938.

379 Abe Y, Liang N, Teramoto M *et al.*, 2022c: Spatial variation in soil respiration rate is
380 controlled by the content of particulate organic materials in the volcanic ash soil under a
381 Cryptomeria japonica plantation. *Geoderma Regional* **29**, e00529.
382 doi:10.1016/j.geodrs.2022.e00529.

383 Adamczyk B, Sietiö OM, Straková P *et al.*, 2019: Plant roots increase both
384 decomposition and stable organic matter formation in boreal forest soil. *Nature*
385 *communications* **10**, 3982. doi:10.1038/s41467-019-11993-1.

386 Behera N, Joshi SK, Pati DP, 1990: Root contribution to total soil metabolism in a
387 tropical forest soil from Orissa, India. *Forest ecology and management* **36**, 125–134.
388 doi:10.1016/0378-1127(90)90020-C.

389 Binkley D, Singer F, Kaye M *et al.*, 2003: Influence of elk grazing on soil properties in
390 Rocky Mountain National Park. *Forest ecology and management* **185**, 239–247.
391 doi:10.1016/s0378-1127(03)00162-2.

392 Bond-Lamberty B, Thomson A, 2010: A global database of soil respiration data.
393 *Biogeosciences* **7**, 1915–1926. doi:10.5194/bg-7-1915-2010.

394 Boone RD, Nadelhoffer KJ, Canary JD *et al.*, 1998: Roots exert a strong influence on
395 the temperature sensitivityof soil respiration. *Nature* **396**, 570–572. doi:10.1038/25119.

396 Bretz F, Hothorn T, Westfall P, 2010: Multiple Comparisons Using R [Computer
397 program]. Available at: https://doi.org/10.1201/9781420010909 (Downloaded: 1 April
398 2023).

399 Ceccon C, Panzacchi P, Scandellari F *et al.*, 2011: Spatial and temporal effects of soil
400 temperature and moisture and the relation to fine root density on root and soil
401 respiration in a mature apple orchard. *Plant and Soil* **342**, 195–206.
402 doi:10.1007/s11104-010-0684-8.

403 Chen FC, Katayama A, Oyamada M *et al.*, 2023: Effects of soil environmental changes
404 accompanying soil erosion on the soil prokaryotes and fungi of cool temperate forests in
405 Southern Japan. *Journal of Forest Research* **29**, 89–102.
406 doi:10.1080/13416979.2023.2265006.

Chen S, Wang J, Zhang T *et al.*, 2020: Climatic, soil, and vegetation controls of the temperature sensitivity (Q_{10}) of soil respiration across terrestrial biomes. *Global Ecology and Conservation* **22**, e00955. doi:10.1016/j.gecco.2020.e00955.

Comeau LP, Lai DYF, Cui JJ *et al.*, 2018: Separation of soil respiration: a site-specific comparison of partition methods. *SOIL* **4**, 141–152. doi:10.5194/soil-4-141-2018.

Coomes DA, Allen RB, Forsyth DM *et al.*, 2003: Factors preventing the recovery of New Zealand forests following control of invasive deer. *Conservation biology* **17**, 450–459. doi:10.1046/j.1523-1739.2003.15099.x.

DEIMS-SDR (2021) *Shiiba Research Forest, Kyushu University - Japan*. Available at: https://deims.org/5a5e3c04-2ed0-42f8-910e-bc41e540248c (Accessed: 15 August 2021).

Deng J, Fang S, Fang X *et al.*, 2023: Forest understory vegetation study: current status and future trends. *Forestry Research* **3**, 6. doi:10.48130/FR-2023-0006.

Enoki T, Kubota K, Kaji K *et al.*, 2017: Effects of sika deer on long-term stand dynamics of Abies-Tsuga forest in the Kyushu mountain range. *Bulleten of the Kyushu University Forest* **98**, 17–24. doi:10.15017/1804318 (Japanese with English summary).

Epron D, Le Dantec V, Dufrene E *et al.*, 2001: Seasonal dynamics of soil carbon dioxide efflux and simulated rhizosphere respiration in a beech forest. *Tree physiology* **21**, 145–152. doi:10.1093/treephys/21.2-3.145.

426 Forbes ES, Cushman JH, Burkepile DE, 2019: Synthesizing the effects of large, wild
427 herbivore exclusion on ecosystem function. *Functional ecology* **33**, 1597–1610.
428 doi:10.1111/1365-2435.13376.

429 Franck N, Morales JP, Arancibia-Avendaño D *et al.*, 2011: Seasonal fluctuations in
430 Vitis vinifera root respiration in the field. *The New phytologist* **192**, 939–951.
431 doi:10.1111/j.1469-8137.2011.03860.x.

432 Guerisoli MLM, Pereira JA, 2020: Deer damage: A review of repellents to reduce
433 impacts worldwide. *Journal of environmental management* **271**, 110977.
434 doi:10.1016/j.jenvman.2020.110977.

435 Han M, Jin G, 2018: Seasonal variations of Q_{10} soil respiration and its components in
436 the temperate forest ecosystems, northeastern China. *European journal of soil biology*
437 **85**, 36–42. doi:10.1016/j.ejsobi.2018.01.001.

438 Harada K, Ang Meng Ann J, Suzuki M, 2020: Legacy effects of sika deer
439 overpopulation on ground vegetation and soil physical properties. *Forest ecology and*
440 *management* **474**, 118346. doi:10.1016/j.foreco.2020.118346.

441 Hernández MPG, Silva-Pando FJ, 1996: Grazing effects of ungulates in a Galician oak
442 forest (northwest Spain). *Forest ecology and management* **88**, 65–70.
443 doi:10.1016/S0378-1127(96)03810-8.

444 Horsley SB, Stout SL, deCalesta DS, 2003: White-tailed deer impact on the vegetation
445 dynamics of a northern hardwood forest. *Ecological applications* **13**, 98–118.
446 doi:10.1890/1051-0761(2003)013[0098:wtdiot]2.0.co;2.

447 Hursh A, Ballantyne A, Cooper L *et al.*, 2017: The sensitivity of soil respiration to soil
448 temperature, moisture, and carbon supply at the global scale. *Global change biology* **23**,
449 2090–2103. doi:10.1111/gcb.13489.

450 Ichihashi R, Katayama A, 2024: Aboveground biomass and structural characteristics of
451 poisonous *Pieris japonica* shrub stands dominating under deer pressure. *Journal of*
452 *Forest Research* **(Online early)**, 1–5. doi:10.1080/13416979.2024.2370065.

453 Iijima H, Nagata J, Izuno A *et al.*, 2023: Current sika deer effective population size is
454 near to reaching its historically highest level in the Japanese archipelago by release from
455 hunting rather than climate change and top predator extinction. *Holocene* **33**, 718–727.
456 doi:10.1177/09596836231157063.

457 Jia B, Zhou G, Wang Y *et al.*, 2006: Effects of temperature and soil water-content on
458 soil respiration of grazed and ungrazed Leymus chinensis steppes, Inner Mongolia.
459 *Journal of arid environments* **67**, 60–76. doi:10.1016/j.jaridenv.2006.02.002.

460 Jian J, Frissell M, Hao D *et al.*, 2022: The global contribution of roots to total soil
461 respiration. *Global ecology and biogeography* **31**, 685–699. doi:10.1111/geb.13454.

462 Jing H, Liu Y, Wang G *et al.*, 2021: Effects of nitrogen addition on root respiration of
463 trees and understory herbs at different temperatures in *Pinus tabulaeformis* forest. *Plant*
464 *and Soil* **463**, 447–459. doi:10.1007/s11104-021-04925-w.

465 Kadowaki K, Honjo MN, Nakamura N *et al.*, 2023: eDNA metabarcoding analysis
466 reveals the consequence of creating ecosystem-scale refugia from deer grazing for the
467 soil microbial communities. *Environmental DNA* **5**, 1732–1742. doi:10.1002/edn3.498.

468 Katayama A, Oyamada M, Abe H *et al.*, 2023: Soil erosion decreases soil microbial
469 respiration in Japanese beech forests with understory vegetation lost by deer. *Journal of*
470 *Forest Research* **28**, 428–435. doi:10.1080/13416979.2023.2235499.

471 Kato M, Okuyama Y, 2004: Changes in the biodiversity of a deciduous forest
472 ecosystem caused by an increase in the sika deer population at Ashiu, Japan.
473 *Contributions from the Biological Laboratory, Kyoto University* **29**, 437–448.

474 Kawakami E, Katayama A, Hishi T, 2020a: Effect of the understory shrub *Pieris*
475 *japonica* on litter decomposition. *Bulleten of the Kyushu University Forest* **101**, 1-6
476 (Japanese with English summary). doi:10.15017/3051274.

477 Kawakami E, Katayama A, Hishi T, 2020b: Effects of declining understory vegetation
478 on leaf litter decomposition in a Japanese cool-temperate forest. *Journal of Forest*
479 *Research* **25**, 260–268. doi:10.1080/13416979.2020.1759884.

480 Kuriyama T, Quoc Huy P, Salmawati S *et al.*, 2021: A Threshold Line for Safe
481 Geologic CO_2 Storage Based on Field Measurement of Soil CO_2 Flux. *C* **7**, 34. doi:
482 10.3390/c7020034.

483 Kooijman AM, Smit A, 2001: Grazing as a measure to reduce nutrient availability and
484 plant productivity in acid dune grasslands and pine forests in The Netherlands.
485 *Ecological engineering* **17**, 63–77. doi:10.1016/S0925-8574(00)00131-2.

486 Leroux SJ, Wiersma YF, Vander Wal E, 2020: Herbivore Impacts on Carbon Cycling in
487 Boreal Forests. *Trends in ecology and evolution* **35**, 1001–1010.
488 doi:10.1016/j.tree.2020.07.009.

Li R, Zheng W, Yang Q *et al.*, 2019: The response of soil respiration to thinning was not affected by understory removal in a Chinese fir (*Cunninghamia lanceolata*) plantation. *Geoderma* **353**, 47–54. doi:10.1016/j.geoderma.2019.06.025.

Lindstrom ML, Bates DM, 1990: Nonlinear mixed effects models for repeated measures data. *Biometrics* **46**, 673–687.

Liu L, Wang X, Lajeunesse MJ *et al.*, 2016: A cross-biome synthesis of soil respiration and its determinants under simulated precipitation changes. *Global change biology* **22**, 1394–1405. doi:10.1111/gcb.13156.

Liu XJA, Finley BK, Mau RL *et al.*, 2020: The soil priming effect: Consistent across ecosystems, elusive mechanisms. *Soil biology and biochemistry* **140**, 107617. doi:10.1016/j.soilbio.2019.107617.

Liu Y, Li J, Hai X *et al.*, 2022: Carbon inputs regulate the temperature sensitivity of soil respiration in temperate forests. *Journal of arid land* **14**, 1055–1068. doi:10.1007/s40333-022-0102-0.

Lloyd J, Taylor JA, 1994: On the temperature dependence of soil respiration. *Functional ecology* **8**, 315–323. doi:10.2307/2389824.

Luan J, Liu S, Wang J *et al.*, 2013: Factors affecting spatial variation of annual apparent Q_{10} of soil respiration in two warm temperate forests. *PloS one* **8**, e64167. doi:10.1371/journal.pone.0064167.

Manzoni S, Schimel JP, Porporato A, 2012: Responses of soil microbial communities to water stress: results from a meta-analysis. *Ecology* **93**, 930–938. doi:10.1890/11-0026.1.

Miguez F, 2021: nlraa: Nonlinear regression for agricultural applications (Version 0.98) [Computer program]. Available at: https://cran.r-project.org/web/packages/nlraa/index.html (Downloaded: 1 April 2022).

Morris KA, Hornum S, Crystal-Ornelas R *et al.*, 2022: Soil respiration response to simulated precipitation change depends on ecosystem type and study duration. *Journal of geophysical research. Biogeosciences* **127**, e2022JG006887. doi:10.1029/2022jg006887.

Niwa S, Mariani L, Kaneko N *et al.*, 2011: Early-stage impacts of sika deer on structure and function of the soil microbial food webs in a temperate forest: A large-scale experiment. *Forest ecology and management* **261**, 391–399. doi:10.1016/j.foreco.2010.10.024.

Ohashi M, Kumagai T, Kume T *et al.*, 2008: Characteristics of soil CO_2 efflux variability in an aseasonal tropical rainforest in Borneo Island. *Biogeochemistry* **90**, 275–289. doi:10.1007/s10533-008-9253-0.

Ohira M, Gomi T, Iwai A *et al.*, 2022: Ecological resilience of physical plant-soil feedback to chronic deer herbivory: Slow, partial, but functional recovery. *Ecological applications* **32**, e2656. doi:10.1002/eap.2656.

Pinheiro J, Bates D, DebRoy S *et al.*, 2017: Package 'nlme.' Linear and nonlinear mixed effects models (Version 3) [Computer program]. Available at: http://mirror.csclub.uwaterloo.ca/CRAN/web/packages/nlme/nlme.pdf (Downloaded: 1 April 2022).

R Core Team, 2024: R: A language and environment for statistical computing (Version 4.2.2 for Windows 10 x64) [Computer program]. Available at: https://www.r-project.org (Downloaded: 1 April 2024).

Ramirez JI, Jansen PA, Poorter L, 2018: Effects of wild ungulates on the regeneration, structure and functioning of temperate forests: A semi-quantitative review. *Forest ecology and management* **424**, 406–419. doi:10.1016/j.foreco.2018.05.016.

Riutta T, Kho LK, Teh YA *et al.*, 2021: Major and persistent shifts in below-ground carbon dynamics and soil respiration following logging in tropical forests. *Global change biology* **27**, 2225–2240. doi:10.1111/gcb.15522.

Rodeghiero M, Cescatti A, 2006: Indirect partitioning of soil respiration in a series of evergreen forest ecosystems. *Plant and Soil* **284**, 7–22. doi:10.1007/s11104-005-5109-8.

Ruehr NK, Buchmann N, 2009: Soil respiration fluxes in a temperate mixed forest: seasonality and temperature sensitivities differ among microbial and root–rhizosphere respiration. *Tree physiology* **30**, 165–176. doi:10.1093/treephys/tpp106.

Ruess RW, Hendrick RL, Bryant JP, 1998: Regulation of fine root dynamics by mammalian browsers in early successional Alaskan taiga forests. *Ecology* **79**, 2706–2720. doi:10.1890/0012-9658(1998)079[2706:rofrdb]2.0.co;2.

Saha S, Huang L, Khoso MA *et al.*, 2023: Fine root decomposition in forest ecosystems: an ecological perspective. *Frontiers in plant science* **14**: 1277510. doi:10.3389/fpls.2023.1277510.

552 Saiz G, Byrne KA, Butterbach-bahl K *et al.*, 2006: Stand age-related effects on soil
553 respiration in a first rotation Sitka spruce chronosequence in central Ireland. *Global*
554 *change biology* **12**, 1007–1020. doi:10.1111/j.1365-2486.2006.01145.x.

555 Sapronov DV, Kuzyakov YV, 2007: Separation of root and microbial respiration:
556 Comparison of three methods. *Eurasian Soil Science* **40**, 775–784.
557 doi:10.1134/S1064229307070101.

558 Saruki S, Inoue S, Shiiba Y *et al.*, 2004: Distribution and growth situation of Suzutake
559 (*Sasamorpha boreal*) damaged by grazing of Shika deer (*Cervus nippon nippon*) in
560 Miyazaki Forest of Kyushu University: Case study in 2003. *Bulleten of the Kyushu*
561 *University Forest* **85**, 47–54 (Japanese with English summary).

562 Schmitz OJ, Wilmers CC, Leroux SJ *et al.*, 2018: Animals and the zoogeochemistry of
563 the carbon cycle. *Science* **362**, eaar3213. doi:10.1126/science.aar3213.

564 Spiess AN, Neumeyer N, 2010: An evaluation of R^2 as an inadequate measure for
565 nonlinear models in pharmacological and biochemical research: a Monte Carlo
566 approach. *BMC pharmacology* **10**, 6. doi:10.1186/1471-2210-10-6.

567 Suzuki M, Miyashita T, Kabaya H *et al.*, 2008: Deer density affects ground-layer
568 vegetation differently in conifer plantations and hardwood forests on the Boso
569 Peninsula, Japan. *Ecological research* **23**, 151–158. doi:10.1007/s11284-007-0348-1.

570 Takatsuki S, 2009: Effects of sika deer on vegetation in Japan: A review. *Biological*
571 *conservation* **142**, 1922–1929. doi:10.1016/j.biocon.2009.02.011.

572 Tang X, Du J, Shi Y *et al.*, 2020: Global patterns of soil heterotrophic respiration – A
573 meta-analysis of available dataset. *Catena* **191**, 104574.
574 doi:10.1016/j.catena.2020.104574.

575 Tape KD, Gustine DD, Ruess RW *et al.*, 2016: Expansion of Moose in Arctic Alaska
576 Linked to Warming and Increased Shrub Habitat. *PloS one* **11**, e0160049.
577 doi:10.1371/journal.pone.0160049.

578 Thurgood A, Singh B, Jones E *et al.*, 2014: Temperature sensitivity of soil and root
579 respiration in contrasting soils. *Plant and Soil* **382**, 253–267. doi:10.1007/s11104-014-
580 2159-9.

581 Tokumoto Y, Katayama A, 2024: Effects of *Pieris japonica* (Ericaceae) dominance on
582 cool temperate forest altered-understory environments and soil microbiomes in
583 Southern Japan. *PloS one* **19**, e0296692. doi:10.1371/journal.pone.0296692.

584 Tokumoto Y, Sakurai Y, Abe H et al., 2024: Effects of deer-exclusion fences on soil
585 microbial communities through understory environmental changes in a cool temperate
586 deciduous forest in Southern Japan. *Forest ecology and management* **564**, 121993.
587 doi:10.1016/j.foreco.2024.121993.

588 Tomotsune M, Yoshitake S, Watanabe S *et al.*, 2013: Separation of root and
589 heterotrophic respiration within soil respiration by trenching, root biomass regression,
590 and root excising methods in a cool-temperate deciduous forest in Japan. *Ecological*
591 *research* **28**, 259–269. doi:10.1007/s11284-012-1013-x.

592 Tremblay JP, Huot J, Potvin F, 2006: Divergent nonlinear responses of the boreal forest
593 field layer along an experimental gradient of deer densities. *Oecologia* **150**, 78–88.
594 doi:10.1007/s00442-006-0504-2.

595 Wang Y, Zhang X, Zhang H *et al.*, 2022: *Dynamic correlation between surface CO_2*
596 *flux and underlying emissions from spontaneous goaf combustion: An experimental*
597 *study of abandoned Coal Mine* [online]. [Preprint]. [Viewed 10 August 2022].
598 Available from: https://www.researchsquare.com/article/rs-1488354/latest.

599 Watanabe T, Fukuzawa K, Shibata H, 2013: Temporal changes in litterfall, litter
600 decomposition and their chemical composition in Sasa dwarf bamboo in a natural forest
601 ecosystem of northern Japan. *Journal of Forest Research* **18**, 129–138.
602 doi:10.1007/s10310-011-0330-1.

603 Webster KL, Creed IF, Skowronski MD *et al.*, 2009: Comparison of the performance of
604 statistical models that predict soil respiration from forests. *Soil Science Society of*
605 *America journal* **73**, 1157–1167. doi:10.2136/sssaj2008.0310.

606 Wilson AD, MacLeod ND, 1991: Overgrazing: present or absent? *Journal of Range*
607 *Management* **44**, 475–482.

608 Yashiro Y, Shizu Y, Adachi T *et al.*, 2012: The effect of dense understory dwarf
609 bamboo (*Sasa senanensis*) on soil respiration before and after clearcutting of cool
610 temperate deciduous broad-leaved forest. *Ecological research* **27**, 577–586.
611 doi:10.1007/s11284-012-0925-9.

612 Zhang S, Yang X, Li D *et al.*, 2022: A meta-analysis of understory plant removal
613 impacts on soil properties in forest ecosystems. *Geoderma* **426**, 116116.
614 doi:10.1016/j.geoderma.2022.116116.

615 Zhao B, Ballantyne AP, Meng S, *et al.*, 2022: Understory plant removal counteracts tree
616 thinning effect on soil respiration in a temperate forest. *Global change biology* **28**,
617 6102–6113. doi:10.1111/gcb.16337.

618 Zhuang W, Liu M, Wu Y *et al.*, 2023: Litter inputs exert greater influence over soil
619 respiration and its temperature sensitivity than roots in a coniferous forest in north-south
620 transition zone. *The Science of The Total Environment* **886**, 164009.
621 doi:10.1016/j.scitotenv.2023.164009.

Tables

Table 1 Mean and standard deviation (SD) of understory vegetation biomass and soil properties in Sasa understory (SU), no understory (NU), and Asebi understory (AU). Different lowercase letters a and b indicate a significant difference (p <0.05, two-sided Tukey honest significant differences test).

Table 2 Estimated constants and their SE as well as SD of random effects (RE). The value of n indicates the number of data points. The model terms T, θ, and T & θ indicated soil temperature, soil volumetric water content, and hybrid of temperature and water models, respectively (see Eqs. 4–6). Values of R^2 are the marginal R^2 of the model.

Table 3 Results of regression analysis for Q_{10} of R_s and R_h. The p values show the significance of the slope value. Results with p <0.05 are shown in boldface. The '+' symbol in the R^2 column indicates a significant positive effect.

635 Table 1

Variables	**SU**	**NU**	**AU**
Understory biomass ($g\ m^{-2}$)	3382.13 ± 728.45 a	128.66 ± 222.84 b	653.7 ± 306.4 b
Surface litter amount ($g\ m^{-2}$)	1197.3 ± 56.9 a	984.1 ± 265.5 a	1011.2 ± 146.1 a
Fine root biomass ($g\ m^{-2}$)			
0–10 cm	215.6 ± 51.7 a	273.9 ± 99.2 a	291.1 ± 155.9 a
0–5 cm	90.6 ± 58.7 a	131.1 ± 23.8 a	186.0 ± 1.0 a
5–10 cm	125.0 ± 88.2 a	142.8 ± 83.5 a	106.1 ± 58.7 a
Soil organic matter ($g\ C\ m^{-2}$)			
0–10 cm	1843.4 ± 253.9 a	2781.0 ± 384.2 b	2412.6 ± 199.6 a
0–5 cm	859.8 ± 199.4 a	1390.0 ± 81.1 b	1258.6 ± 202.6 a
5–10 cm	983.8 ± 57.69 a	1391.0 ± 322.7 a	1154.1 ± 75.5 a
Soil bulk density ($g\ cm^{-3}$)			
0–5 cm	64.8 ± 19.0 a	94.9 ± 6.5 a	76.9 ± 12.5 a
5–10 cm	94.1 ± 17.8 a	135.4 ± 37.7 a	92.7 ± 3.1 a
Soil carbon concentration (%)			
0–5 cm	16.1 ± 2.1 a	17.6 ± 1.7 a	19.7 ± 1.7 a
5–10 cm	12.8 ± 1.8 a	12.4 ± 0.6 a	14.9 ± 0.5 a

636

637 Table 2

Sasa understory (SU)				No understory (NU)				Asebi understory (AU)			
	Fixed effect		SD of RE		Fixed effect		SD of RE		Fixed effect		SD of RE
	Constant	SE			Constant	SE			Constant	SE	
R_s (n = 1809)				**R_s (n = 1782)**				**R_s (n = 2331)**			
T (AIC = -5439.92, R^2 = 0.84)				***T*** (AIC = -2835.64, R^2 = 0.87)				***T*** (AIC = -4597.95, R^2 = 0.89)			
a	0.16	0.018	0.032	a	0.16	0.022	0.037	a	0.12	0.016	0.027
b	0.089	0.0062	0.011	b	0.092	0.0038	0.0064	b	0.10	0.0060	0.010
θ (AIC = 825.26, R^2 = 0.15)				***θ*** (AIC = 945.19, R^2 = 0.31)				***θ*** (AIC = -42.54, R^2 = 0.23)			
c	6.30	0.63	2.1×10^{-15}	c	-7.7	1.7	2.7	c	5.0	3.0	5.1
d	-0.66	0.12	0.16	d	1.7	0.11	0.14	d	-0.58	0.35	0.60
f	0.019	0.0058	0.0093	f	-0.032	0.0018	2.4×10^{-9}	e	0.018	0.010	0.017
T* & *θ (AIC = -5611.54, R^2 = 0.88)				***T* & *θ*** (AIC = -2833.64, R^2 = 0.86)				***T* & *θ*** (AIC = -4589.92, R^2 = 0.89)			
g	0.36	0.079	0.13	g	0.15	0.016	8.2×10^{-15}	g	0.11	0.017	0.026
h	0.089	0.0044	0.0076	h	0.091	0.0032	0.0053	h	0.10	0.0060	0.010
i	-0.28	0.075	0.13	i	0.019	0.055	0.075	i	0.0091	0.024	3.2×10^{-9}
R_h (n = 1720)				**R_h (n = 1873)**				**R_h (n = 2170)**			
T (AIC = -4964.31, R^2 = 0.92)				***T*** (AIC = -4176.56, R^2 = 0.91)				***T*** (AIC = -5548.52, R^2 = 0.89)			
a	0.096	0.0030	0.0048	a	0.072	0.016	0.028	a	0.051	0.0059	0.010
b	0.10	0.0013	0.0020	b	0.11	0.010	0.017	b	0.12	0.0058	0.010
θ (AIC = -1829.85, R^2 = 0.49)				***θ*** (AIC = 467.82, R^2 = 0.043)				***θ*** (AIC = -830.63, R^2 = 0.015)			
c	4.6	1.6	2.7	c	-0.40	0.42	0.34	c	-0.44	0.22	0.30
d	-0.41	0.20	0.35	d	0.13	0.040	7.7×10^{-9}	d	0.093	0.021	0.021
f	0.010	0.0062	0.011	f	-0.0044	0.0012	0.00094	f	-0.0027	0.00055	8.2×10^{-9}
T* & *θ (AIC = -4080.78, R^2 = 0.93)				***T* & *θ*** (AIC = -4277.68, R^2 = 0.92)				***T* & *θ*** (AIC = -5523.07, R^2 = 0.90)			
g	0.19	0.016	4.2×10^{-10}	g	0.33	0.046	0.079	g	0.069	0.0060	5.7×10^{-12}
h	0.097	0.0010	1.5×10^{-7}	h	0.11	0.0094	0.016	h	0.12	0.0044	0.0075
i	-0.21	0.026	6.3×10^{-7}	i	-0.53	0.026	0.040	f	-0.11	0.044	0.055

638

639 Table 3

Variables	R_s		R_h	
	R^2	p	R^2	p
Understory biomass (g m^{-2})	0.055	0.54	0.13	0.33
Surface litter amount (g m^{-2})	0.030	0.65	**0.59 +**	**0.015**
Fine root biomass (g m^{-2})				
0–10 cm	**0.69 +**	**0.0060**	0.00	0.99
0–5 cm	**0.47 +**	**0.041**	0.015	0.98
5–10 cm	0.26	0.16	0.014	0.76
Soil organic matter amount (g C m^{-2})				
0–10 cm	0.096	0.42	0.26	0.16
0–5 cm	0.21	0.22	0.25	0.17
5–10 cm	0.0060	0.84	0.19	0.24
Soil bulk density (g cm^{-3})				
0–5 cm	0.30	0.13	0.074	0.48
5–10 cm	0.0050	0.86	0.16	0.29
Soil carbon concentration (%)				
0–5 cm	0.00	0.96	0.21	0.22
5–10 cm	0.010	0.80	0.010	0.80

640

641 **Figures**

642 Fig. 1. Understory vegetation types at the study site in southern Kyushu Island, Japan.
643 Panel (a) shows dwarf bamboo (Sasa; *Sasamorpha borealis*) understory (SU). Panel (b)
644 shows no understory (NU). Panel (c) shows unpalatable shrub, Asebi (*Pieris japonica*)
645 understory (AU).

646 Fig. 2. Response of soil respiration efflux (μmol m^{-2} s^{-1}) to soil temperature at 0–5 cm
647 depth. Data points represent total soil respiration (R_s) and heterotrophic respiration (R_h).
648 Symbols (circles, triangles, and squares) indicate the different measurement points. The
649 solid line indicate the regression line obtained from the fixed effect of the non-linear
650 mixed-effect model with random effects as replicates of the measurement points. The
651 dotted line indicate the regression line at each measurement point (i.e., fixed effect +
652 point-specific random effect).

653 Fig. 3. Relationships between surface litter amount and Q_{10} of R_h. Data points represent
654 the results for each measurement point. Symbols represent understory types. The solid
655 line indicates the significant regression line, and the gray area indicates the 95%
656 confidence interval.

657 Fig. 4. Relationships between fine root biomass at 0–10 cm depth and Q_{10} of R_s. Data
658 points represent the results for each measurement point. Symbols represent understory
659 types. The solid line indicates the significant regression line, and the gray area indicates
660 the 95% confidence interval.

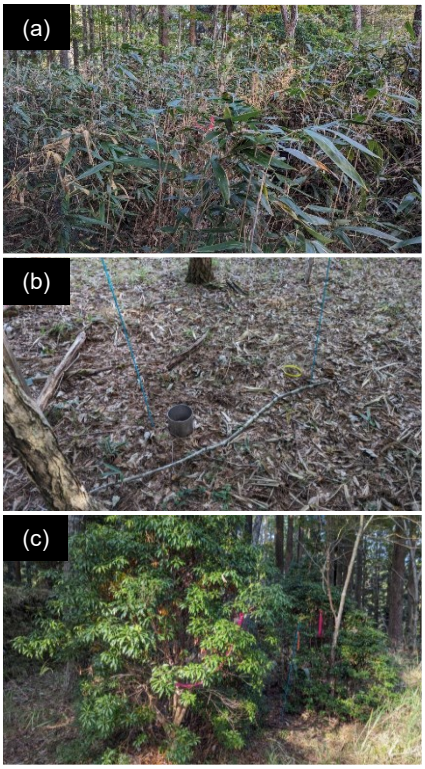

661 Fig. 1.

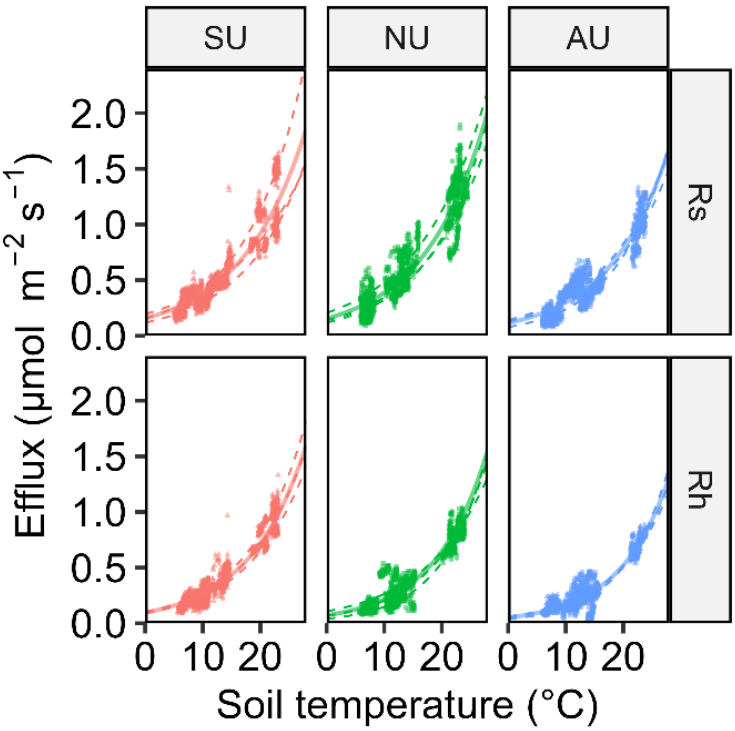
SU
NU
AU
Rs
Rh
Efflux (μmol m^{-2} s^{-1})
2.0
1.5
1.0
0.5
0.0
0 10 20
Soil temperature (°C)

662 Fig. 2.

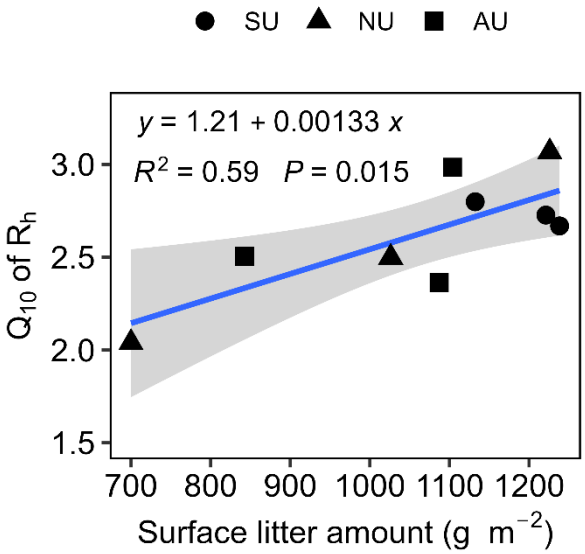
SU
NU
AU
y = 1.21 + 0.00133 x
R2 = 0.59 P = 0.015
Q10 of Rh
3.0
2.5
2.0
1.5
700
800
900
1000
1100
1200
Surface litter amount (g m−2)

663 Fig. 3.

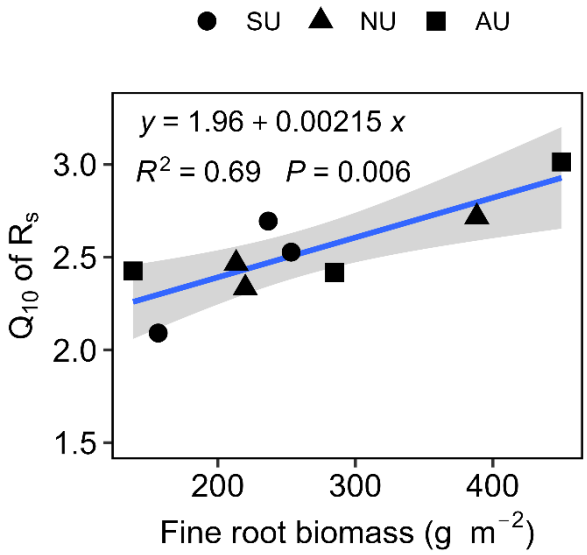
SU
NU
AU
y = 1.96 + 0.00215 x
R2 = 0.69 P = 0.006
3.0
2.5
2.0
1.5
Q10 of Rs
200
300
400
Fine root biomass (g m−2)

664 Fig. 4.

Supplement Table S1: Raw data of Q_{10} and soil properties at each measurement point.

The following data is in tab-delimited format. Please duplicate the data in a spreadsheet or txt file.

Understory type	Point replication	Q10_Rs	Q10_Rh	Understory biomass	Surface litter amount	Fine root biomass	SOM	Mean BD	Mean SC
	Surface litter_tree	Surface litter_sasa	Surface litter_asebi	Surface litter_Inseparatable	Fine root biomass 0-5 cm	Fine root_tree_0-5 cm	Fine root_sasa_0-5 cm	Fine root_asebi_0-5 cm	Fine root biomass 5-10 cm
Fine root_tree_5-10 cm	Fine root_sasa_5-10 cm	Fine root_asebi_5-10 cm	SOM 0-5 cm	SOM 5-10 cm	BD 0-5 cm	BD 5-10 cm	SC 0-5 cm	SC 5-10 cm	
SU	#1	2.5	2.7	2555.4	1238.3	253.3	1889	77.6	15.3
1174.3	11.1	0	52.9	28.3	23.3	5	0	225	
141.7	83.3	0	914.2	974.8	59.6	95.6	18.4	12.2	
SU	#2	2.7	2.8	3661.4	1132.3	236.7	2071.4	98.5	12.8
1107.1	25.2	0	0	145	111.7	33.3	0	91.7	
70	21.7	0	1026	1045.3	85.8	111.1	14.3	11.3	
SU	#3	2.1	2.7	3929.6	1221.1	156.7	1569.8	62.2	15.2
1122.8	62.2	0	36.1	98.3	83.3	15	0	58.3	
31.7	26.7	0	638.6	931.2	48.9	75.5	15.7	14.8	
NU	#1	2.5	2.5	0	1026.2	213.3	2469.4	101	14.6
1026.2	0	0	0	136.7	136.7	0	0	76.7	
76.7	0	0	1376.8	1092.6	102.3	99.8	16.1	13.1	
NU	#2	2.7	3.1	386	1226	388.3	2663.3	111.5	14.8
1226	0	0	0	151.7	151.7	0	0	236.7	
236.7	0	0	1316.3	1347	91.4	131.7	17.3	12.3	
NU	#3	2.3	2	0	700	220	3210.3	132.8	15.7
700	0	0	0	105	105	0	0	115	
115	0	0	1476.9	1733.4	90.9	174.8	19.5	11.9	
AU	#1	2.4	3	971.1	1103.8	138.3	2212	79.2	17.1
932.1	0	49.4	122.2	96.7	21.7	0	75	41.7	
30	0	11.7	1026.9	1185.2	65.6	92.8	18.8	15.3	

697	AU	#2	3	2.5	630.2	842.8	450	2611.3	93.1	16.9
698		678.8	0	94.7	69.3	293.3	141.7	0	151.7	156.7
699		73.3	0	83.3	1402.2	1209	90.3	95.8	18.6	15.1
700	AU	#3	2.4	2.4	359.7	1087.1	285	2414.6	82.2	18
701		556.4	0	105.3	425.3	165	90	0	75	120
702		76.7	0	43.3	1346.6	1068	74.7	89.6	21.6	14.3

Supplement figures

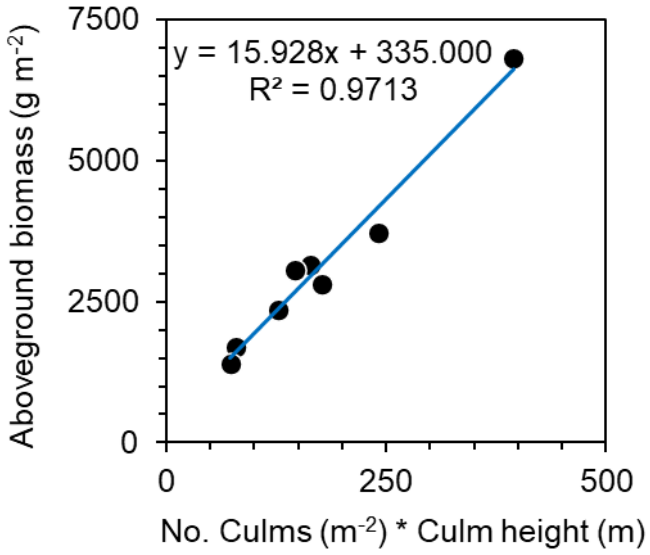

Fig. S1. Relationships between aboveground Sasa biomass (g m^{-2}) and multipliers for culm height (m) and number of Sasa culms (m^{-2}). Data are obtained from Abe *et al.* (2024b).

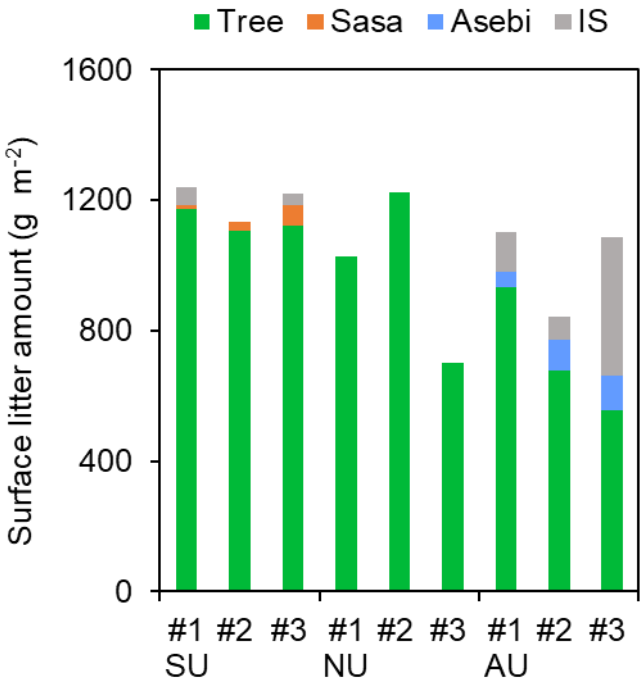

Fig. S2. Surface litter amount and its species composition in each CO_2 efflux measurement point. Abbreviations for category: Tree; overstory trees, Sasa; dwarf bamboo (*Sasamorpha borealis*), Asebi; unpalatable shrubs (*Pieris japonica*), and IS; litters that have decomposed and become inseparable. Abbreviation for understory types: SU; Sasa understory, NU; no understory, and AU; Asebi understory.

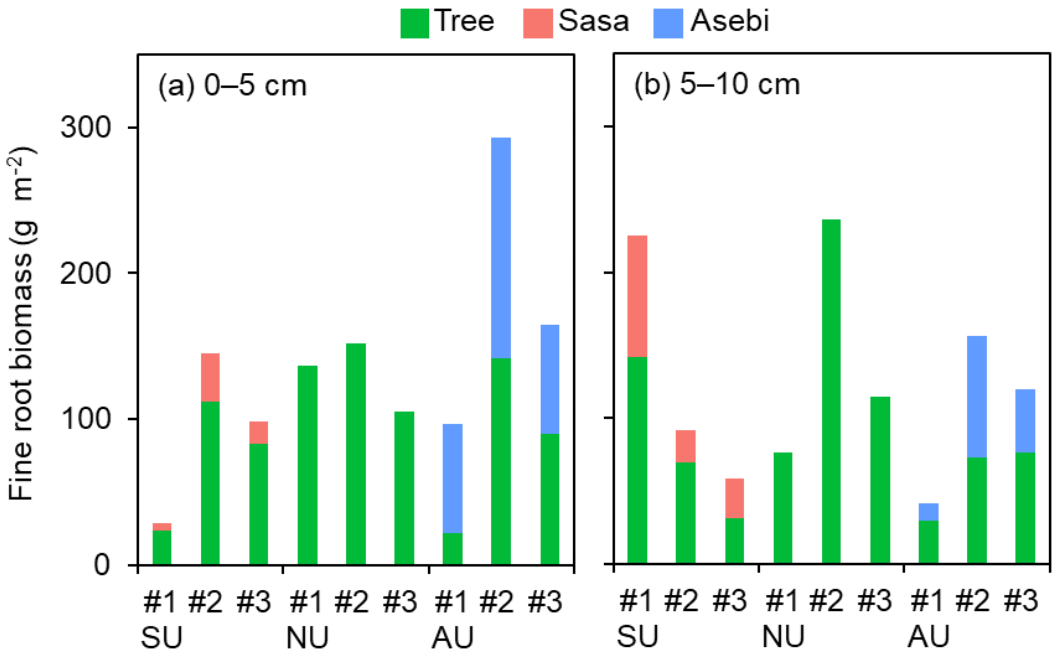

713 **Fig. S3.** Fine root biomass at its species composition at 0–5 cm (a) and 5–10 cm depth

714 (b).

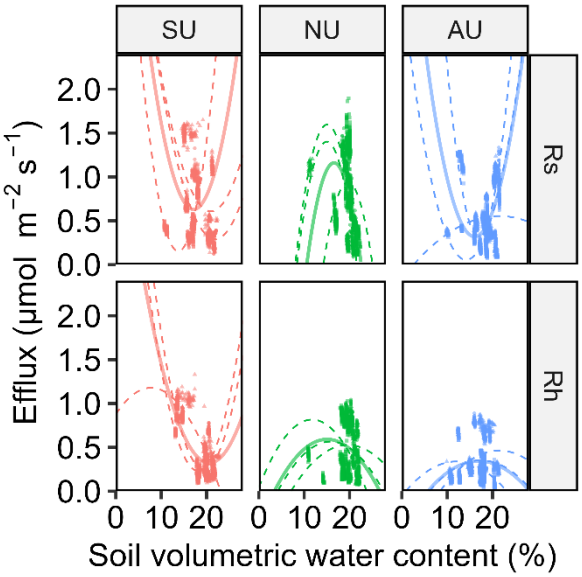

Fig. S4. Response of soil respiration efflux (μmol m^{-2} s^{-1}) to soil volumetric water content. Dots represent total soil respiration (R_s) and heterotrophic respiration (R_h). Symbols of dots (circles, triangles, and squares) indicate the different measurement points. The solid lines indicate regression lines obtained from the fixed effect of the non-linear mixed effect model with random effects as replicates of the measurement points. The dotted lines indicate the regression lines at each measurement point (i.e., fixed effect + point-specific random effect).

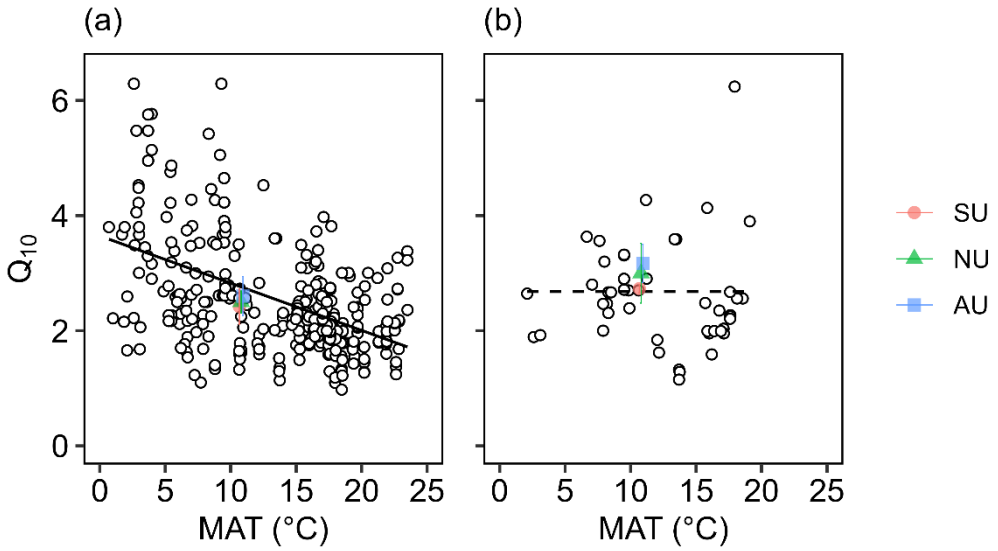

722 **Fig. S5.** Temperature sensitivity (Q_{10}) of R_s (a) and R_h (b) to mean annual temperature
723 (MAT) in forest ecosystems. Open dots indicate literature data obtained from Chen *et*
724 *al.* (2020). Filled dots indicate the results of SU, NU, and AU in the present study.
725 Although MAT in SU, NU, and AU are the same (10.8 ℃), these dots are drawn
726 slightly offset for ease of viewing. The solid line in panel (a) shows a regression line
727 between Q_{10} of R_s and MAT (Q_{10} = 3.70 −0.0848*MAT, adjusted R^2 = 0.23, $p < 0.001$)
728 based on the literature data sets. The dotted line in panel (b) shows the mean of the
729 overall average of the data sets (Q_{10} = 2.7) because the regression line is not significant
730 (p = 0.614). Note that literature data from Chen *et al.* (2020) used only Q_{10} which was
731 created using soil temperature at 5 cm depth, and excluded three outliers (Q_{10} >10).